

The Roton in a Bose-Einstein Condensate

J. Steinhauer¹, R. Ozeri², N. Katz², and N. Davidson²

¹*Department of Physics, Technion Israel Institute of Technology, Technion City, Haifa 32000, Israel and*

²*Department of Physics of Complex Systems, Weizmann Institute of Science, Rehovot 76100, Israel*

The roton in a Bose-Einstein condensate is computed, both near and far from a Feshbach resonance. A low-density approximation is made, allowing for an analytic result. A Monte Carlo calculation shows that the roton is larger than predicted by the low-density approximation, for the upper range of densities considered here. The low-density approximation is applied to superfluid ⁴He, roughly reproducing the results of previous Monte Carlo calculations.

PACS numbers:

A roton, first predicted by Landau [1] for superfluid ⁴He, is an excitation in a Bose-Einstein condensed fluid, characterized by a minimum in the excitation spectrum $\omega(k)$. By Feynman's relation [2], this minimum also corresponds to a maximum in the static structure factor $S(k)$. This peak in $S(k)$ occurs for excitations whose wavelength $2\pi/k$ is equal to the characteristic wavelength of density fluctuations in the ground-state wave function of the quantum fluid. The peak in $S(k)$ exceeds unity, the value for an uncorrelated gas.

Feynman [2] described several possible microscopic pictures of a roton in superfluid ⁴He. He found that the most likely description is that the roton is analogous to a single atom moving through the condensate, with wave number k close to $2\pi/n^{-1/3}$, where $n^{-1/3}$ is the mean atomic spacing.

The roton in superfluid ⁴He was calculated by a Monte Carlo technique [3, 4] using a many-body Jastrow wave function [5], which is of the form

$$\psi = \prod_{j>i=1}^N f(|\mathbf{r}_i - \mathbf{r}_j|), \quad (1)$$

where the pair function $f(r)$ should be determined for the quantum fluid under consideration. The wave function (1) deviates significantly from unity if any two atoms become very close to one another. For superfluid ⁴He, the two-particle correlation function $g(r)$ for this wave function has fluctuations with a preferential length scale of $n^{-1/3}$, which results in a peak greater than unity in $S(k)$ near $k \approx 2\pi/n^{-1/3}$, in agreement with Feynman's picture.

Both Feynman's result and the results of the Jastrow wave function roughly agree with measurements [6] of $S(k)$ and $\omega(k)$.

The Jastrow wave function (1) has also been considered for a low-density Bose-Einstein condensate (BEC) [3], and has been used to compute various properties of a high-density BEC [7]. We employ a Jastrow wave function to compute the roton for a low-density BEC. By an analytic calculation, we find that the hard-sphere size r_o of the atoms determines the location of the roton, rather than $n^{-1/3}$. We see that Feynman's view that $n^{-1/3}$

is the relevant length scale is the special case of high-density, for which $r_o \approx n^{-1/3}$.

In a low-density BEC, Feynman's view of the roton as a single atom moving through the condensate seems natural. In general, the excitation spectrum of a low-density BEC is of the Bogoliubov form [8, 9], which consists of phonons and single-particle excitations. We find that the roton occurs on the single-particle part of the spectrum, at $k \approx 8/\pi a$, where a is the s -wave scattering length.

Although the general form of the wave function (1) can be applied to both superfluid ⁴He and BEC, the wave function is fundamentally different for these two quantum fluids. For both of these fluids, below some temperature $T_{s\text{-wave}}$, the thermal de-Broglie wavelength λ_{dB} becomes longer than the characteristic length scale R of the interparticle potential. Below $T_{s\text{-wave}}$, all scattering processes except for s -wave scattering become negligible. Since a BEC is a dilute gas, $n^{-1/3}$, which is typically about 1500\AA , is much larger than R . Therefore, the critical temperature T_c for quantum degeneracy, at which λ_{dB} becomes comparable to $n^{-1/3}$, is much lower than $T_{s\text{-wave}}$. Therefore, only s -wave scattering plays a role here for a BEC. In contrast to BEC, superfluid ⁴He is a relatively dense liquid, for which $n^{-1/3}$ is comparable to R . Therefore, the temperature $T_{s\text{-wave}}$ also marks the transition T_c to quantum degeneracy. Even below T_c for superfluid ⁴He, partial waves other than the s -wave contribute to the wave function.

For many properties of a BEC, a is sufficient to describe the interparticle potential, and the form of the potential does not play a role [10, 11]. To quantitatively describe the roton however, the s -wave scattering wave function must be known to interparticle separations somewhat smaller than R , where the details of the potential are relevant.

Rotons have been predicted in a BEC in the presence of optical fields [12, 13], as well as in a dipolar BEC [14]. In this work, we find that a roton occurs in an unperturbed BEC without any dipole interaction. We consider the enhancement of the roton near a Feshbach resonance [15, 16], but the physics is qualitatively the same as in the unperturbed case.

When we refer to a roton, we are referring to a peak in

$S(k)$, rather than a minimum in $\omega(k)$. By the Feynman relation, the peak in $S(k)$ computed here for a BEC is not steep enough to produce a minimum in $\omega(k)$, for the range of densities considered here.

We use a low-density approximation [5] to compute $g(r)$ and the roton for a BEC with a positive scattering length. The low-density approximation is compared to a Monte Carlo calculation.

For a BEC of alkali atoms, the potential can be taken as the van der Waals potential $-C_6/r^6$ for atomic separations r greater than a few Angstroms [17, 18]. For this potential, R is given by $(mC_6/\hbar^2)^{1/4}$, which ranges from about 50 to 100 Å [18, 19]. The wave function for s -wave scattering between two particles in the limit of zero energy is given by $\psi_6(r)$, which is the solution of the radial Schrödinger equation with the van der Waals potential. $\psi_6(r)$ can be written in terms of elliptic integrals [17]. For $r > R$, this wave function is very close in form to $1 - a/r$ [10, 20]. For the case of $a \gg R$, $\psi_6(r)$ therefore obtains large negative values for $r \ll a$ [21].

We cannot use $\psi_6(r)$ as $f(r)$ in (1), because even for $r \gg n^{-1/3}$, $\psi_6(r)$ is significantly less than unity. This is non-physical, in the sense that no matter how large the gas for fixed density, the value of the many-body wave function (1) depends on the size of the gas. To account for many-body effects, we use the following pair function which goes to unity for $r > n^{-1/3}$ [7, 18].

$$f(r) = \begin{cases} \psi_6(r)/\psi_6(n^{-1/3}) & (r \leq n^{-1/3}) \\ 1 & (r > n^{-1/3}). \end{cases} \quad (2)$$

To compute (2), R is needed. Throughout this work, we use $R = 0.05 n^{-1/3}$. This is a typical experimental value, and the results here are rather insensitive to R .

Equation (1) with (2) is shown schematically in Fig. 1. To aid in visualization, Fig. 1 shows the wave function squared in one dimension, as a function of the position x_1 of atom number 1. The positions of all of the other atoms, such as atoms b through e , are fixed. As long as atom number 1 is far from the other atoms, the wave function has the constant value ψ_0 . This value is determined by the positions of the atoms other than x_1 . The rapid oscillations in $\psi_6(r)$ for $r < R$ appear in Fig. 1 as dark vertical bands, when atom number 1 is very close to another atom.

The correlation function $g(r)$ gives the unconditional probability of two atoms being at a distance r . $g(r)$ is related to the pair function $f(r)$ by [5]

$$g(|\mathbf{r}_1 - \mathbf{r}_2|) = V^2 \frac{\int d\mathbf{r}_3 \dots d\mathbf{r}_N \prod_{j>i=1}^N f^2(|\mathbf{r}_i - \mathbf{r}_j|)}{\int d\mathbf{r}_1 \dots d\mathbf{r}_N \prod_{j>i=1}^N f^2(|\mathbf{r}_i - \mathbf{r}_j|)}, \quad (3)$$

where the integrals are over the volume V . (3) can be evaluated starting with the first integral in the denomi-

nator, $\int d\mathbf{r}_1 \prod_{j>1}^N f^2(|\mathbf{r}_1 - \mathbf{r}_j|)$. This can be visualized as the integral over the function shown in Fig. 1 for one dimension. Neglecting three-body interactions greatly simplifies this integral. Three-body interactions are rare for small values of the gas parameter na^3 , assuming that the range of three-body interactions is of the same order of magnitude as the range of two-body interactions. A three-body interaction is represented in Fig. 1 by the points x_c and x_d , where atoms 1, c , and d interact. Neglecting such interactions, the integral is a function of the volume v indicated by the shaded region in Fig. 1. The integral is then given by $V - (N - 1)v$, where $v = V - \int d\mathbf{r} f^2(r)$. This result is independent of the positions of the \mathbf{r}_j .

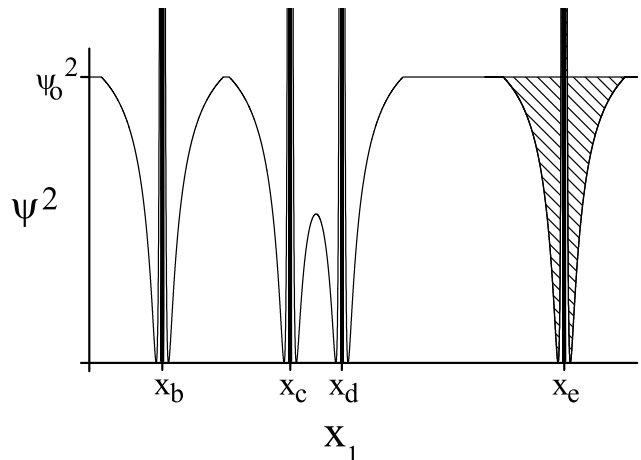


FIG. 1: Schematic one-dimensional representation of the Jastrow wave function. The dependence on the single dimension x_1 is shown. The overall scaling of the curve is given by the factors in the wave function not involving x_1 . The labeled values of x_1 correspond to the positions of atoms other than atom 1. x_1 varies over the volume V .

Evaluating all of the integrals in (3) similarly to the first yields $g(|\mathbf{r}_1 - \mathbf{r}_2|) \approx V^2 f^2(|\mathbf{r}_1 - \mathbf{r}_2|) [(V - v)V]^{-1}$. Since $V \gg v$, we obtain the result of the low-density approximation [5]

$$g(r) \approx f^2(r). \quad (4)$$

The result (4) with (2) is indicated by the solid curve in Fig. 2 for $na^3 = 2.2 \times 10^{-4}$. This value of na^3 is an order of magnitude greater than typical experimental values without a Feshbach resonance. The result for $na^3 = 0.011$ is also shown in the figure.

While (4) is useful for obtaining analytic results, a more accurate computation can be made by the Monte Carlo technique described in Ref. [3]. This technique effectively evaluates (3) by using a Metropolis algorithm to randomly choose configurations of the N atoms ($N = 100$ here), according to the probability distribution given by

(1) with (2), and computing the distribution of distances between the atoms, with periodic boundary conditions. This distribution, averaged over many likely configurations, is proportional to $r^2 g(r)$. The result of the Monte Carlo computation is shown in Fig. 2 for $na^3 = 2.2 \times 10^{-4}$ and 0.011. These results were obtained with 9×10^8 and 2×10^7 iterations, respectively.

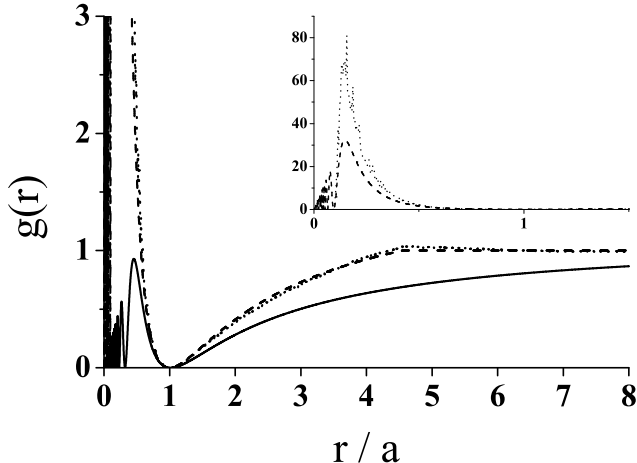


FIG. 2: The two-particle correlation function for a BEC. The solid and dashed curves are the low-density approximation (4) with (2), with $na^3 = 2.2 \times 10^{-4}$ and 0.011, respectively. The dotted curve is the Monte Carlo result for $na^3 = 0.011$. For $na^3 = 2.2 \times 10^{-4}$, the Monte Carlo result is indistinguishable from the solid curve. The inset shows the curves for $na^3 = 0.011$ only.

The small oscillations for small r shown in Fig. 2 are negligible in the computation of the static structure factor. These are the oscillations for r values less than that of the first large peak below $r/a = 1$, in the solid and dashed curves. To save computing time these oscillations are not included in $f^2(r)$ in the Monte Carlo computation.

For $a \geq 1.3R$ (corresponding to $na^3 > 2.7 \times 10^{-4}$ in this work), The peak in $f^2(r)$ located at $r < R$ is greater than unity. The dashed line of the inset of Fig. 2 shows an example of such a peak, for $a = 4.4R$. Because this peak is greater than unity, a cluster of atoms is the most likely configuration. Since we are interested in the un-clustered phase, we do not let the Monte Carlo computation proceed long enough for the clear transition to clusters to occur.

The static structure factor $S(k)$ is given by $1 + n \int [g(r) - 1] e^{i\mathbf{k} \cdot \mathbf{r}} d\mathbf{r}$, which in general can be written

$$S(k) = 1 + 4\pi n \int_0^\infty dr r^2 [g(r) - 1] \frac{\sin(kr)}{kr}. \quad (5)$$

We use (5) to compute $S(k)$ for the low-density approximation (4) with (2), as indicated in Fig. 3. The height

$S(k_r)$ and location k_r of the roton are indicated by the solid curves of Fig. 4. $S(k)$ in Fig. 3 has several maxima, the tallest of which is taken as the roton. As na^3 is varied, the peak which is taken as the roton varies, resulting in the jagged appearance of the solid curves of Fig. 4.

For the Monte Carlo computation, $S(k)$ is found by inserting $g(r)$ such as is shown in Fig. 2 into (5). The results are indicated in Fig. 3 by the dash dotted and solid curves. For small na^3 , the height and location of the roton are seen in Fig. 4 to be the same for the low-density approximation and the Monte Carlo result. The low-density approximation is therefore valid for small na^3 . For the larger values of na^3 , the height of the roton in the Monte Carlo calculation is larger than that of the low-density approximation, as seen in Fig. 4a.

By applying the low-density approximation to the limit of $a \gg R$, we can obtain an analytic expression for $S(k)$ for $R \ll a \ll n^{-1/3}$. In this range, $f(r)$ can be taken as $1 - a/r$. By (4) and (5),

$$S(k) = 1 + 4\pi na^3 [\pi(ka)^{-1}/2 - 2(ka)^{-2}]. \quad (6)$$

This small- R limit is indicated by the dotted curve in Fig. 3. The height of the roton in this limit is $S(k_r) = 1 + \pi^3 na^3/8$, and the location is given by $k_r = 8/\pi a$. These values are indicated by the dashed curves of Fig. 4, which as expected, agree with the low-density approximation (solid curves) for $a \gg R$, where nR^3 is indicated by the dotted lines. As seen in the above expression for k_r , the location of the roton is determined by a , rather than by $n^{-1/3}$.

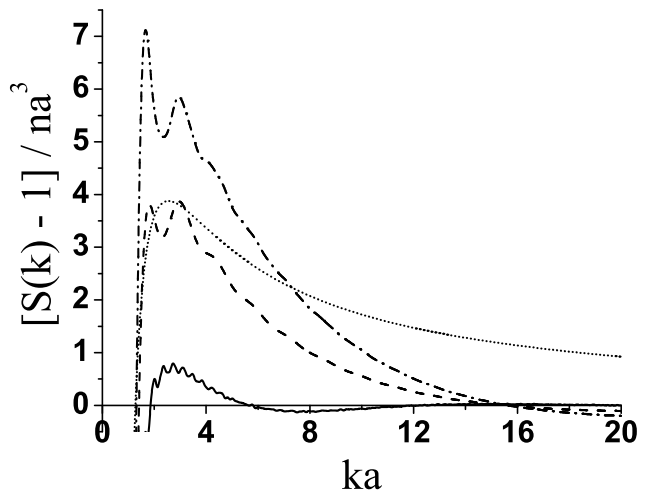


FIG. 3: The roton in a BEC, computed by (5). The dash dotted and solid curves are the Monte Carlo results for $na^3 = 0.011$ and 2.2×10^{-4} respectively. The result of the low-density approximation (4) with (2) for $na^3 = 0.011$ is indicated by the dashed curve. The result of the low-density approximation for $na^3 = 2.2 \times 10^{-4}$ is indistinguishable from the solid curve. The dotted curve is the small- R limit, given by (6).

For $na^3 = 0.011$, the height of the roton given by the

Monte Carlo calculation is $S(k_r) = 1.08$, as shown in Figs. 3 and 4a. Measuring this 8% effect could be experimentally feasible. $na^3 = 0.011$ could be attained by a Feshbach resonance [20]. It should be noted though, that for this relatively large value of na^3 , the form of (2) is only approximate, so the expressions for the height and location of the roton should be considered as estimates only.

Due to phonons, the true $S(k)$ is proportional to k for $k \lesssim \xi^{-1}$, where $\xi^{-1} = a^{-1}\sqrt{8\pi na^3}$ is the inverse healing length. The curves shown in Fig. 3 do not show this linear behavior for small k because the wave function (1) with (2) does not have the long-range correlations of a phonon [3, 4].

For superfluid ${}^4\text{He}$ the three inverse length scales $2\pi/n^{-1/3}$, k_r , and ξ^{-1} , are roughly equal. This is also true for a strong roton in a BEC. As na^3 increases, both k_r and ξ^{-1} approach $2\pi/n^{-1/3}$. More precisely, the ratios of ξ^{-1} and k_r to $2\pi/n^{-1/3}$ are $\sqrt{2/\pi}(na^3)^{1/6}$ and approximately $4/\pi^2(na^3)^{-1/3}$, respectively. The latter ratio implies that an appropriate measurement system for measuring a roton should be able to probe wavelengths somewhat shorter than $n^{-1/3}$.

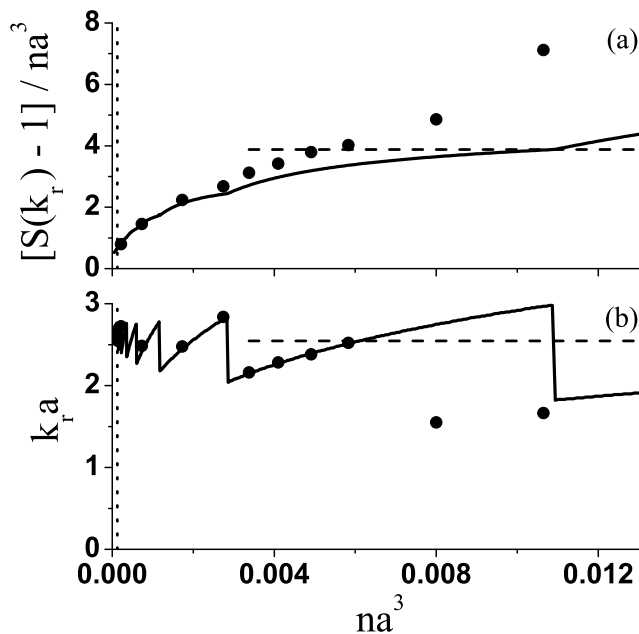


FIG. 4: The height (a) and location (b) of the roton in a BEC, as a function of na^3 . The circles are the Monte Carlo result. The solid curves are the low-density approximation. The dashed curves are the analytic small-R limit. The dotted lines indicate nR^3 .

As a demonstration of the validity of the low-density approximation (4), we use (4) to compute various properties of superfluid ${}^4\text{He}$ found in [3] and [4] by means of Monte Carlo calculations. For superfluid ${}^4\text{He}$, $nb^3 \approx 0.4$ where b is the hard-sphere size. Therefore, this is a strin-

gent test of the low-density approximation. We find that the location of the roton for superfluid ${}^4\text{He}$ is given by $k_r = 5.3/b$, which differs from the Monte Carlo result by 6% [3, 4]. We find that the height of the roton for superfluid ${}^4\text{He}$ is $S(k_r) \approx 1 + 0.3nb^3$, which gives a roton of $S(k_r) = 1.1$, compared to $S(k_r) = 1.2$ from the Monte Carlo calculation [3, 4], and $S(k_r) = 1.5$ from experiment [6]. The order-of-magnitude agreement between the low-density approximation and the Monte Carlo result for superfluid ${}^4\text{He}$ suggests that the low-density approximation preserves the essence of (3).

In conclusion, we find the height $S(k_r)$ and location k_r of a roton in a BEC, for a range of densities. A low-density approximation is compared to a Monte Carlo calculation. The values of $S(k_r)$ and k_r given by the two methods agree for the lowest densities. For higher densities, the Monte Carlo calculation predicts an enhancement in $S(k_r)$ of almost a factor of 2 over the low-density approximation.

In contrast to the Monte Carlo calculation for superfluid ${}^4\text{He}$, the small-R limit gives explicit expressions for the height and location of the roton.

We thank Servaas Kokkelmans, Ady Stern, Yoseph Imry, Daniel Kandel, Johnny Vogels, and Ananth Chikkatur for helpful discussions. This work was supported by the Israel Science Foundation. J. S. is a Landau Fellow, supported by the Taub and Shalom Foundations.

-
- [1] L. Landau, J. Phys. U.S.S.R. **11**, 91 (1947).
 - [2] R. P. Feynman, Phys. Rev. **94**, 262 (1954).
 - [3] W. L. McMillan, Phys. Rev. **138**, 442 (1965).
 - [4] D. Schiff & L. Verlet, Phys. Rev. **160**, 208 (1967).
 - [5] R. Jastrow, Phys. Rev. **98**, 1479 (1955).
 - [6] D. G. Henshaw, Phys. Rev. **119**, 9 (1960). For additional references, see [3], [4], or [10].
 - [7] S. Cowell, H. Heiselberg, I. E. Mazets, J. Morales, V. R. Pandharipande, and C. J. Pethick, Phys. Rev. Lett. **88**, 210403 (2002).
 - [8] N. N. Bogoliubov, J. Phys. (USSR) **11**, 23 (1947).
 - [9] J. Steinhauer, R. Ozeri, N. Katz, and N. Davidson, Phys. Rev. Lett. **88**, 120407 (2002).
 - [10] K. Huang, *Statistical Mechanics* (John Wiley & Sons, 1987).
 - [11] F. Dalfovo, S. Giorgini, L. P. Pitaevskii, and S. Stringari, Rev. Mod. Phys. **71**, 463 (1999).
 - [12] J. Higbie and D. M. Stamper-Kurn, Phys. Rev. Lett. **88**, 090401 (2002).
 - [13] D. H. J. O'Dell, S. Giovanazzi, and G. Kurizki, Phys. Rev. Lett. **90**, 110402 (2003).
 - [14] L. Santos, G. V. Shlyapnikov, and M. Lewenstein, Phys. Rev. Lett. **90**, 250403 (2003).
 - [15] Herman Feshbach, Ann. Phys. **5**, 357 (1958).
 - [16] S. Inouye, M. R. Andrews, J. Stenger, H.-J. Miesner, D. M. Stamper-Kurn, and W. Ketterle, Nature (London) **392**, 151 (1998).
 - [17] G. F. Gribakin and V. V. Flambaum, Phys. Rev. A **48**, 546 (1993).

- [18] A. J. Leggett, *Rev. Mod. Phys.* **73**, 307 (2001).
- [19] M. Marinescu, H. R. Sadeghpour, and A. Dalgarno, *Phys. Rev. A* **49**, 982 (1994).
- [20] Using the formalism of S. J. J. M. F. Kokkelmans, J. N. Milstein, M. L. Chiofalo, R. Walser, and M. J. Holland, *Phys. Rev. A* **65**, 053617 (2002), we find that a is well-defined close to a Feshbach resonance, for the values of a considered here, and for the collisional energies found in the ground state of a BEC.
- [21] J. Dalibard, chapter in *Proceedings of the International School of Physics «Enrico Fermi» Course CXL* (IOS Press, 1999).